

Supplementary Information

Mediation of Donor-Acceptor Distance in An Enzymatic Methyl Transfer Reaction

Jianyu Zhang, Heather J. Kulik, Todd J. Martinez, Judith P. Klinman

Detailed Materials and Methods

Chemicals and reagents were purchased at the highest purity available and used without further purification otherwise indicated. Dopamine was from Acros Organics; dopamine [phenyl-2,5,6-³H] (Specific activity: 30 Ci/mmol) was from ViTrax Inc.; S-adenosyl-L-[methyl-³H] methionine (specific activity: 70.8 Ci/mmol) was from MP Biomedicals LLC.; S-[carboxyl-¹⁴C] adenosyl-L-methionine (specific activity: 55mCi/mmol) was from American Radiolabeled Chemicals Inc. The cocktail for liquid scintillation counting was ECOLITE(+)TM LSC from MP Biomedicals LLC. Other materials such as buffers, salts, general reagents, and culture media were from Fisher Scientific Inc. or VWR except where indicated. The concentration of dopamine ($\lambda_{\max} = 280 \text{ nm}$, $\epsilon = 2,570 \text{ M}^{-1}\text{cm}^{-1}$) and S-adenosyl-L-methionine ($\lambda_{\max} = 260 \text{ nm}$, $\epsilon = 15,400 \text{ M}^{-1}\text{cm}^{-1}$) in solution were determined spectrophotometrically using a Cary50 Bio spectrophotometer.

Expression and Purification of Human Catechol *O*-Methyltransferase (COMT)(1-3)

The expression and purification of the soluble form of COMT and mutants were performed as previously with some modifications.(4) The plasmid sample of human COMT (108V) in the Novagen pET22b(+) vector with a C-terminal histidine tag was a generous gift from Prof. William W. Parson (University of Washington, Seattle). All mutants of COMT were obtained as in a previous study(4) using a commercial kit (QuickChange site-directed mutagenesis kit, Stratagene). Recombinant COMTs were transformed and expressed in *Escherichia coli* BL21 (DE3) cells (Stratagene). Transformed BL21 (DE3) cells were grown in LB medium containing ampicillin (100

$\mu\text{g/ml}$) at 37°C . When the absorbance at 600 nm was around 0.6, cells were induced with 1mM IPTG (Isopropyl β -D-1-thiogalactopyranoside) and grown at 20°C overnight while shaking at 200 rpm. The cells were harvested via centrifugation at $5,000\times g$ for 20 min at 4°C . The cell pellets were re-suspended in 100 mM TrisHCl (pH 8), 0.3 M NaCl, 1 mM EDTA, 20% glycerol (v/v), 10 mM β -mercaptoethanol, 5 mM MgCl_2 with lysozyme (1 mg/ml) and incubated on ice for 30min. The suspended solution was sonicated, adding phenylmethylsulfonyl fluoride (PMSF, 0.1M) in advance. After lysis, the cells were centrifuged at $20,000\times g$ for 20 min at 4°C . In order to eliminate the AdoMet generated in the expression, the clear supernatant was incubated at 37°C for 1 h with 1 μM GNMT (glycine *N*-methyltransferases) and 20 mM glycine. Then the reaction mixture was cooled in ice and applied to a pre-equilibrated Ni-NTA metal affinity column (QIAGEN). The column was washed with at least 50-column volumes of wash buffer (100 mM NaPO_4 (pH 8), 0.4 M NaCl, 20% glycerol (v/v), 10 mM β -mercaptoethanol, 5 mM MgCl_2 , and 20 mM imidazole). COMT was collected by using elution buffer (100 mM NaPO_4 (pH 7.4), 0.25 M NaCl, 20% glycerol (v/v), 5 mM β -mercaptoethanol, 5 mM MgCl_2 , and 100 mM imidazole) and concentrated. The concentrated solution was applied to a Sephacryl S-200 HiPrep 26/60 size column and the pure COMT was obtained and dialyzed against dialysis buffer (elution buffer without imidazole). Finally, the protein was concentrated and stored at -80°C until further use. Protein concentrations were calculated using the Bradford assay.

Stability of the AdoMet in the Presence of Enzyme

The mixture of AdoMet (final concentration around 40 μM), trace S-adenosyl-L-

[methyl-³H] methionine, and COMT enzyme (final concentration around 50 μM) were incubated at 37°C in 100 mM phosphate buffer (pH 6.8) with 5 mM MgCl₂, 4 mM 1,4-dithiothreitol. At different time points, 50 μL aliquots were removed and quenched by 5 μL 4M HClO₄. The samples were centrifuged and loaded onto HPLC with a C18 column (Luna 5 μ C18 100A from Phenomenex). The AdoMet was eluted by mixture of a 12.5% acetonitrile, 10 mM 1-heptane sulfonic acid sodium salt and 50 mM phosphate at pH 2.5 and collected for scintillation counting. The result shows that the presence of the COMT enzyme stabilizes the AdoMet for at least 5 h at 37°C (Figure S11).

Competitive Equilibrium Binding Isotope effect (BIE) Measurement

The mixture of S-adenosyl-L-[methyl-³H] methionine and S-[carboxyl-¹⁴C] adenosyl-L-methionine (CPM ratio for ³H:¹⁴C is around 4:1) was applied to an HPLC system based on C18 reversed phase column (Kinetex™ 5 μm, 100 Å, 250×4.6 mm from Phenomenex) and then eluted by 50mM ammonium formate buffer (pH=4.0), followed by 50mM ammonium acetate buffer (pH=5.4) with 1% TFA and finally 10 mM Phosphate buffer (pH=6.8)(5). Fractions at the AdoMet elution time were collected and concentrated and stored in freezer for further use. Metal-free, sterile Spectra/Por 2 dialysis membrane (MWCO:12-14k) were prepared by 3 circles of boiling in 2% (w/v) sodium bicarbonate and 1 mM EDTA for 15 min and distilled water for another 15 min, finally stored in 20% ethanol solution at 4°C. The prepared wet dialysis membrane was sandwiched between two halves of an ultrafiltration apparatus (from Vern L. Schramm in Albert Einstein College of Medicine of Yeshiva University) and dried at room temperature in vacuum for 2-3 days. The binding isotope effects (BIEs) were measured

using the ultrafiltration method described by the Schramm group. (6-9) The solution (320 μL) for the measurement consisted of 50 μM recombinant COMT protein, the mixture of above purified S-adenosyl-L-[methyl- ^3H] methionine and S-[carboxyl- ^{14}C] adenosyl-L-methionine in 100 mM phosphate buffer with 5 mM MgCl_2 , 4 mM 1,4-dithiothreitol (pH 6.8), and incubated for 15 min at room temperature. Three 100 μL aliquots were removed and added to the upper wells of the ultrafiltration apparatus, and around 22 psi nitrogen gas (N_2) was applied for 50 min, at which time around half of the solution had passed through the dialysis membrane into the lower well. Samples (25 μL) from the top and bottom wells were taken by using a Hamilton syringe into a 20 mL scintillation vial with 500 μL distilled water. A 5 g scintillation cocktail was added to each sample, which was analyzed by liquid scintillation counter (Packard Tri-Carb 2700TR) for at least ten cycles (10 min per cycle). The counting channels for ^3H and ^{14}C are 0-12 eV and 35-156 eV, respectively. The BIEs were calculated from equation S1(6, 7), where $^{14}\text{C}_{\text{top}}$ and $^3\text{H}_{\text{top}}$ are the counts for the ^{14}C and ^3H in the top wells, respectively, and $^{14}\text{C}_{\text{bottom}}$ and $^3\text{H}_{\text{bottom}}$ are the counts for the ^{14}C and ^3H in the bottom wells, respectively. The BIEs and errors were calculated from independent replicates on different days.

$$\text{BIE} = \frac{{}^{14}\text{C}_{\text{top}}/{}^{14}\text{C}_{\text{bottom}} - 1}{{}^3\text{H}_{\text{top}}/{}^3\text{H}_{\text{bottom}} - 1} \quad (\text{Suppl. Eq. 1})$$

Competitive Primary (1°) KIE Measurements

The primary KIE for COMT were determined as previous.(4) Briefly, the mixture consisted of the recombinant COMT protein, 5 mM MgCl_2 , 4 mM 1,4-dithiothreitol, 50 μM AdoMet (with S-adenosyl-L-[methyl- ^{14}C] methionine 27,000 cpm/nmol), and 100 μM dopamine (with [phenyl-2,5,6- ^3H]-dopamine 80,000 cpm/nmol) in phosphate buffer (50 mM, pH 6.8). The reaction mixture was preincubated at 37°C and was initiated by the

addition of the recombinant human COMT protein. At different time points, 50 μL aliquots were removed and quenched by 5 μL 4M HClO_4 . Concentrated WT COMT was added to the reaction mixture to achieve 100% conversion (t_∞) of AdoMet, and more than five t_0 and t_∞ values were obtained. Independent experiments were carried out three times for each mutant to obtain the KIE. The quenched aliquots were stored at -20°C prior to separation by HPLC. The samples were loaded onto a HPLC system based on a C18 column (Luna 5 μ C18 100A from Phenomenex). The solvent system consisted of a mixture of 12.5% acetonitrile, 10 mM 1-heptane sulfonic acid sodium salt and 50 mM phosphate at pH 2.5. The isolated dopamine, AdoMet, 3-*O*-methyldopamine and 4-*O*-methyldopamine were analyzed by liquid scintillation counter (Packard Tri-Carb 2700TR). The KIE was calculated according to equation S2,(10-12) where f is the fractional extent of the reaction, and R_t and R_∞ are the isotope ratios of $^3\text{H}/^{14}\text{C}$ at times t and infinity, respectively.

$$\text{KIE} = \frac{\ln(1 - f)}{\ln\left(1 - f \frac{R_t}{R_\infty}\right)} \quad (\text{Suppl. Eq. S2})$$

Competitive Secondary (2°) KIE Measurements

The secondary KIE was determined in a similar way as the primary KIE, except that the pattern of labeling and the initial amount of radioactivity in the AdoMet and dopamine were different. The final concentration of AdoMet was constant ($[\text{C}] = 50 \mu\text{M}$) with [methyl- ^3H]-AdoMet (220,000 cpm/nmol), and the concentration of dopamine was varied: 100 μM , 200 μM , 400 μM and 800 μM with [8- ^{14}C] dopamine 27,000 cpm/nmol. In this way, comparable counts could be obtained for the isolated product but with larger background counts as more labeled dopamine was used with increasing [dopamine].

Results are summarized in Table S1.

Dissociation constant (Kd) Measurements

The dissociation constants (Kd) for binding of AdoMet to COMT and its mutants were measured by fluorescence quenching titration (13). Measurements were carried out in 100 mM phosphate buffer (pH 7.4) with 5 mM MgCl₂, 4 mM 1,4-dithiothreitol at 37°C on a custom built Fluorolog-3 spectrofluorometer (Horiba Jobin-Yvon) and excitation was achieved with a 450W xenon lamp. The excitation wavelength was set at 291 nm, and the emission spectra were collected from wavelengths spanning 300–400 nm at 1 nm increments. Fluorescence peak intensities were collected as a function of changing AdoMet concentration and were used to calculate the dissociation constant (Kd) of the binary complexes (COMT-AdoMet) according to equation S3:

$$Y=(F_0-X)*K_d/(X-F_{in})+(F_0-X)*[E]/(F_0-F_{in}) \quad (\text{Suppl. Eq. 3})$$

where Y is [AdoMet] concentration, X is fluorescence intensity, F₀ is the fluorescence intensity when no AdoMet is added, F_{in} is the intensity extrapolated to infinite AdoMet concentration, and [E] is the protein concentration.

Time-Resolved Fluorescence Measurements

All techniques, instrument specifications, and subsequent downstream analyses of TRES, Stokes shifts, and fluorescence lifetimes were described and performed as previously reported from this laboratory with minor modification(14). The emission monochromator was set at 291 nm in the same buffer as the Kd measurements at 37°C. Fluorescence decays of the single-Trp variants were obtained from 335–365 nm in 5 nm

intervals with a 10 nm emission bandpass.

Calculations of the Equilibrium Isotope Effect

Equilibrium isotope effect calculations were carried out for the reaction of free AdoMet and deprotonated catecholate reactants by obtaining the zero-point energy of the protium and tritium-substituted reactant and products using vibrational analysis implemented in the DLFIND package or Gaussian 09(15). These calculations were carried out at ω PBEh/6-31+g* or B3LYP/6-31+g** with a polarizable continuum model (IEFPCM) for solvent. Subsequent force constant calculations were performed, frequencies were computed for isotopologues of interest, and the resulting frequencies were used to calculate the EIE. The results are assembled in Table S7.

Overall Protein Simulation Preparation

We simulated the 214-residue, 3419 atom soluble, human form of COMT² starting from available crystal structures (PDB ID: 3BWM). Six residues at the C terminus and one residue at the N terminus of the protein are unresolved in the crystal structure. The protein was crystallized in the presence of a dinitrocatechol inhibitor, which we replaced with a catecholate anion substrate in our simulations. Mutants (Y68A and Y68F) were prepared in PyMOL using the mutagenesis tool on the crystal structure of the protein and simulated using the same parameters as those employed in the current and previous studies of the WT enzyme. Three water molecules resolved in the crystal structure that were buried in the interior of the active site near the catalytically relevant Mg²⁺ ion were preserved in the simulation setup. This system was protonated and solvated using tleap in a truncated icosahedron box that provided at least 10 Å additional water buffer.

MM Molecular Dynamics Calculations

For all simulations, we first carried out extensive molecular mechanics (MM) molecular dynamics simulations with AMBER 14(16). A combined minimization, NVT heating, and NPT equilibration was carried out for 5 ns. Then production runs to collect statistics on SAM(C)-catecholate(O⁻) distances were collected for a minimum of an additional 80 ns. These simulations used the ff9SB AMBER force field and the TIP3P water model for solvent. Generalized amber force field (GAFF) parameters for the catecholate and SAM were generated from RESP charges (HF/6-31G*) and the parameter generation codes available with AMBER. The entire system was solvated using a truncated icosahedron periodic boundary conditions with a box of 10 Å of TIP3P water. Both mutants and wildtype were equilibrated as follows: 1) restrained minimization step with frozen protein for 1000 steps, 2) free minimization for 1000 steps, 3) quick 20 ps heating stage (NVT ensemble), 4) equilibration at constant 1 bar pressure and 300 K (NPT) with standard pressure coupling constant for 5 ns, 5) production in NVE for 80-150 ns (upper range is for WT). Calculations were carried out using the GPU-accelerated PMEMD code. In all cases, a 1fs timestep was used without SHAKE on the protein and therefore hydrogens were flexible. This study departs from previous MM MD studies, which were carried out only with NVE equilibration, with a shorter 1 ns timescale for total simulation time, and with bonding constraints on the Mg²⁺ that enforced bonding to neighboring proteins, catecholate, and a water molecule.

QM/MM Calculations

A representative snapshot from the median C-O distance observed in MM dynamics was used as the starting point for our combined quantum mechanical (QM) and molecular

mechanics (MM) approach (QM/MM). For QM/MM we use our TeraChem package(17) for the QM portion and AMBER 14 for the molecular mechanics force field component. When we transition from pure MM to QM/MM dynamics, we cut out a sphere of maximum radius from the center of mass (typically 34 Å) and re-equilibrate the MM waters for 1 ns with the protein held fixed. This transition to spherical boundary conditions is required because our QM/MM method does not support periodic boundary conditions for the QM interaction with MM point charges. The QM region is modeled with density functional theory using the range-separated exchange-correlation functional ω PBEh within the 6-31g(18) basis set. We have previously benchmarked this approach for protein structure(19).

The QM region was chosen based on observations from previous studies of convergence of catalytic and electronic structure properties(20). This QM region consists of all residues within 5 Å of the AdoMet and catecholate reactants and directly incorporates all residues that were observed experimentally to have a significant role on catalytic efficiency (E6, W38, Y68, W143, K144). In each model, any residue not included in the QM region is automatically treated with a MM force field description. The net charge of all residues included in this QM region is -2, while the total charge on the protein is determined to be -6, assuming pH 7. Neutralizing Na⁺ charges were added using the tleap program in the AMBER package(16) and employed in both the pure MM dynamics and QM/MM optimizations. Structural optimizations were carried out for the QM/MM simulations using steepest descent followed by conjugate gradient, as implemented in the QM/MM interface in AMBER.

Table S1. The secondary tritium kinetic isotope effect (2° KIE) for the methyl transfer from AdoMet [50 μ M] to different concentration of dopamine, catalyzed by WT human COMT.

[Dopamine], μ M	100	200	400	800
2° KIE ^a	0.791 \pm 0.012	0.782 \pm 0.038	0.783 \pm 0.056	0.812 \pm 0.071

^aThese are $k_{\text{CH}_3}/k_{\text{CT}_3}$. The trend in errors with increasing dopamine is due to the larger background uncertainty when more radioactive-labeled substrate is added to achieve similar counting statistics in the product.

Table S2. The primary [¹⁴C] kinetic isotope effect and kinetic parameters for the methyl transfer from AdoMet to dopamine, catalyzed by the recombinant human COMT and its mutants.

COMT	1° KIE ^a	Relative values for k_{cat}/K_m (Dopamine) ^c
108V(WT)	1.063 ± 0.020 ^b	757
Y68F	1.071 ± 0.017	115
Y68A	1.120 ± 0.035	2
V108M	1.065 ± 0.033 ^b	1,238
V108M/Y68F	1.070 ± 0.021	126
V108M/Y68A	1.145 ± 0.051	1

^aThis is $k(^{12}\text{C})/k(^{14}\text{C})$. ^bData from ref. 4. ^cThe lowest catalytic efficiency is set to unity, as a frame of reference. Original data from ref. 4.

Table S3. Kinetic Parameters for WT, Y68F and Y68A mutants as well as single-Trp variants: W143in, W143in/Y68F and W143in/Y68A.

COMT	k_{cat} (min^{-1})	$k_{\text{cat}}/K_{\text{m}}(\text{M}^{-1}\text{s}^{-1})$	$k_{\text{cat}}/K_{\text{m}}(\text{M}^{-1}\text{s}^{-1})$
		AdoMet ^a	Dopamine ^a
WT	12.3±0.3	3,200±360 (72)	833±55 (320)
Y68F	21.9±0.9	1,370±230(30)	127±14 (49)
Y68A	0.81±0.05	45±7 (1)	2.6±0.2 (1)
W143in	15.1±1.1	1,830±440 (1,304)	38.1±6.9 (79)
W143in/Y68F	17.2±2.8	960±380 (686)	8.7±2.7 (18)
W143in/Y68A	0.14±0.10	1.4±1.0 (1)	0.48±0.36 (1)

^aIn the bracket, the lowest catalytic efficiency is set to unity for compare.

Table S4. Representative fluorescence decay parameters for W143in, W143in/Y68F and W143in/Y68A in apo form and in binary complex (with AdoMet).^a

COMT	α_1	τ_1 (ns)	α_2	τ_2 (ns)	α_3	τ_3 (ns)	$\langle\tau\rangle$ (ns) ^b
Apo-COMT							
W143in			0.17	2.10	0.83	6.45	5.72
W143in/Y68F			0.15	2.21	0.85	6.69	6.02
W143in/Y68A			0.14	2.30	0.86	6.36	5.79
COMT Binary Complex							
W143in	0.28	0.37	0.18	1.92	0.53	6.37	3.85
W143in/Y68F	0.08	0.44	0.17	2.45	0.75	6.75	5.52
W143in/Y68A	0.10	0.38	0.17	2.25	0.73	6.48	5.16

^a Lifetimes were obtained at 350nm. α_i and τ_i were obtained by fitting two or three exponential functions for apo- and holo-COMT with standard deviation lower than 5%, respectively. No sub-nanosecond lifetimes were observed for apo-COMT series. ^b $\langle\tau\rangle = \sum \alpha_i \tau_i$.

Table S5. X-ray structures of ternary complexes of COMT^a.

PDB ID	Source	Inhibitor used	Resolution,Å	C•••O Distance^b	Reference
1VID	Rat	Figure S7 a	2.00	2.6 Å	(1994) Nature 368 : 354-358
1HID	Rat	Figure S7 b	2.00	2.8 Å	(2002) Mol.Pharmacol. 62 : 795
2CL5	Rat	Figure S7 c	1.60	2.7 Å	(2006) Mol.Pharmacol. 70 : 143
3BWY	Human/108M	Figure S7 a	1.30	2.7 Å	(2008) J.Mol.Biol. 380 : 120-130
3BWM	Human	Figure S7 a	1.98	2.7 Å	(2008) J.Mol.Biol. 380 : 120-130
2ZVJ	Rat	Figure S7 d	2.30	2.8 Å	(2009) Biochem.Biophys.Res.Commun. 378 : 494-497
3A7E	Human	Figure S7 a	2.80	2.6 Å	2010No ref, Deposit only
3S68	Rat	Figure S7 e	1.85	2.5 Å	(2012) Acta Crystallogr.,Sect.D 68 : 253-260

^a The complexes refer to the COMT crystals with AdoMet and inhibitor. ^b The distance is the carbon of methyl group in AdoMet to catechol inhibitor oxygen, measured by Pymol.

Table S6. Hydrogen bonding distance (C–H···O) between the carbon atom of the methyl group in AdoMet and oxygen atom of Asp141 or main chain carbonyl oxygen of Met40 in binary COMT complex (PDB: 2ZTH structure only) and ternary COMT complex (all other structures). Units in Å.

PDB ID	Resolution	C-D141 OB	C-D141 OD1	C- D141 OD2	C-M40 O
1VID	2.00	3.3	3.9	3.7	3.5
1HID	2.00	3.6	3.9	4.1	3.2
2CL5	1.60	3.4	4.0	3.8	3.4
3BWY	1.30	3.3	3.9	3.7	3.4
3BWM	1.98	3.2	3.8	3.8	3.3
2ZVJ	2.30	3.3	4.0	4.1	3.5
3A7E	2.80	3.0	3.6	3.6	3.6
3S68	1.85	3.3	3.8	3.8	3.3
2ZTH	2.60	3.6	4.6	4.5	-

Table S7. Computed equilibrium isotope effects in water for the methyl group transfer from AdoMet to a range of catechol anions.

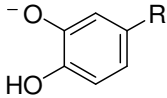
	ω PBEh/6-31+g*	B3LYP/6-31+g**
Dopamine (R=CH ₂ CH ₂ NH ₃ ⁺)	0.837	0.829
2-hydroxyphenol (R=H)	0.815	–
L-DOPA (R=CH ₂ CH(NH ₂)COOH)	0.830	–

Figure S1. Kinetic Reaction Mechanism for COMT.

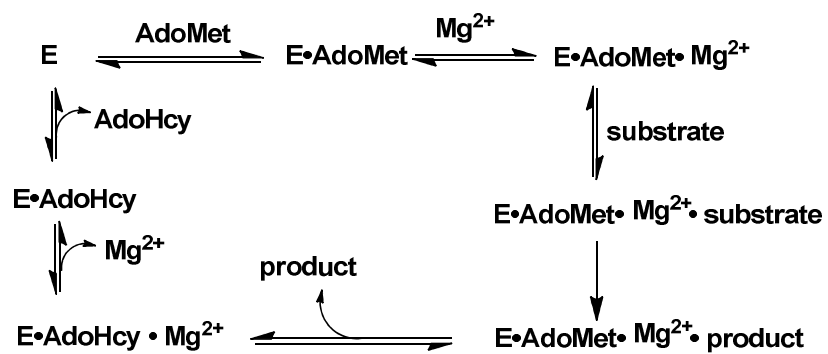


Figure S2. Methyl transfer reaction by COMT via S_N2 mechanism.

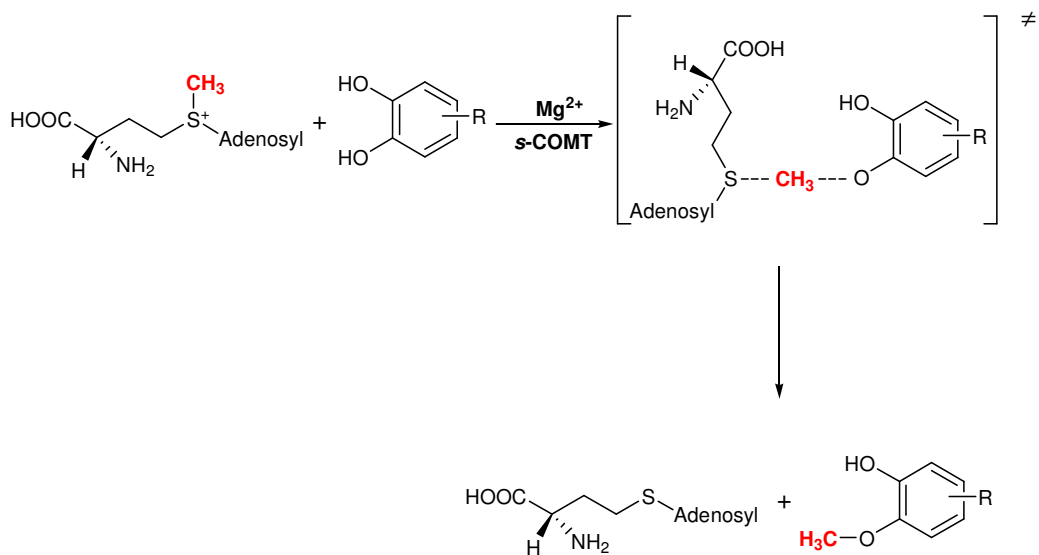
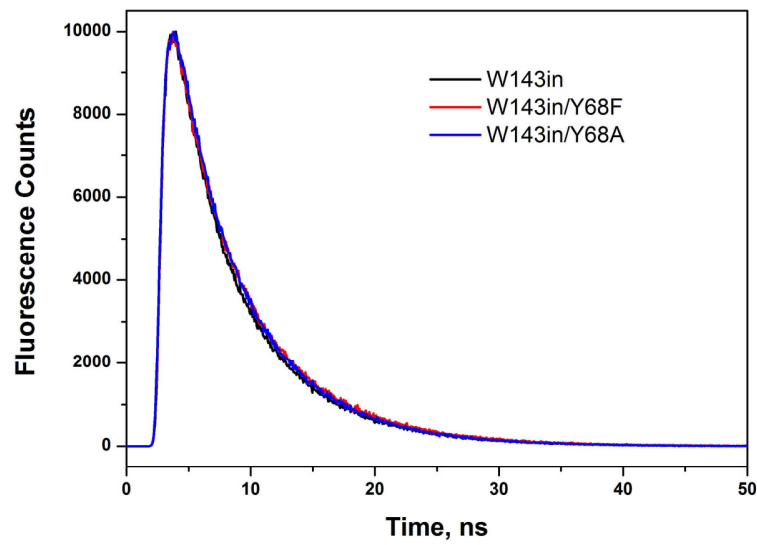


Figure S3. Experimentally observed fluorescence transients of W143in (black), W143in/Y68F (red) and W143in/Y68A(blue) at 350nm for (a) apo-COMT, (b) AdoMet-COMT.

(a)



(b)

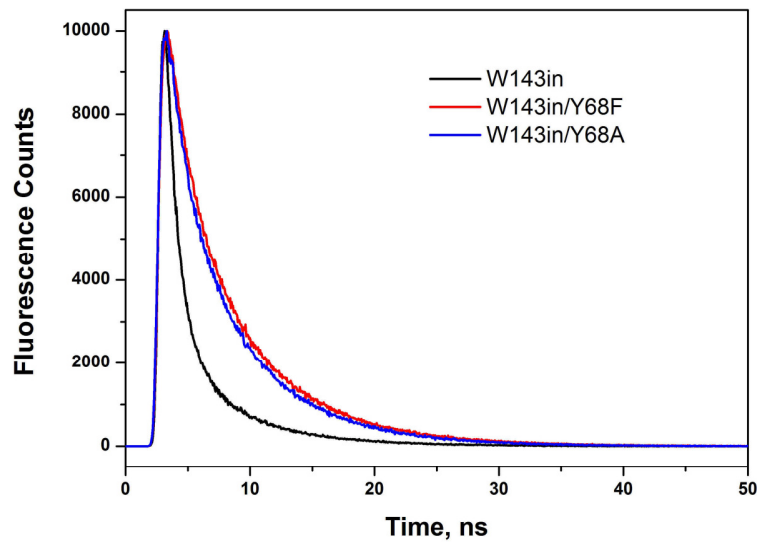
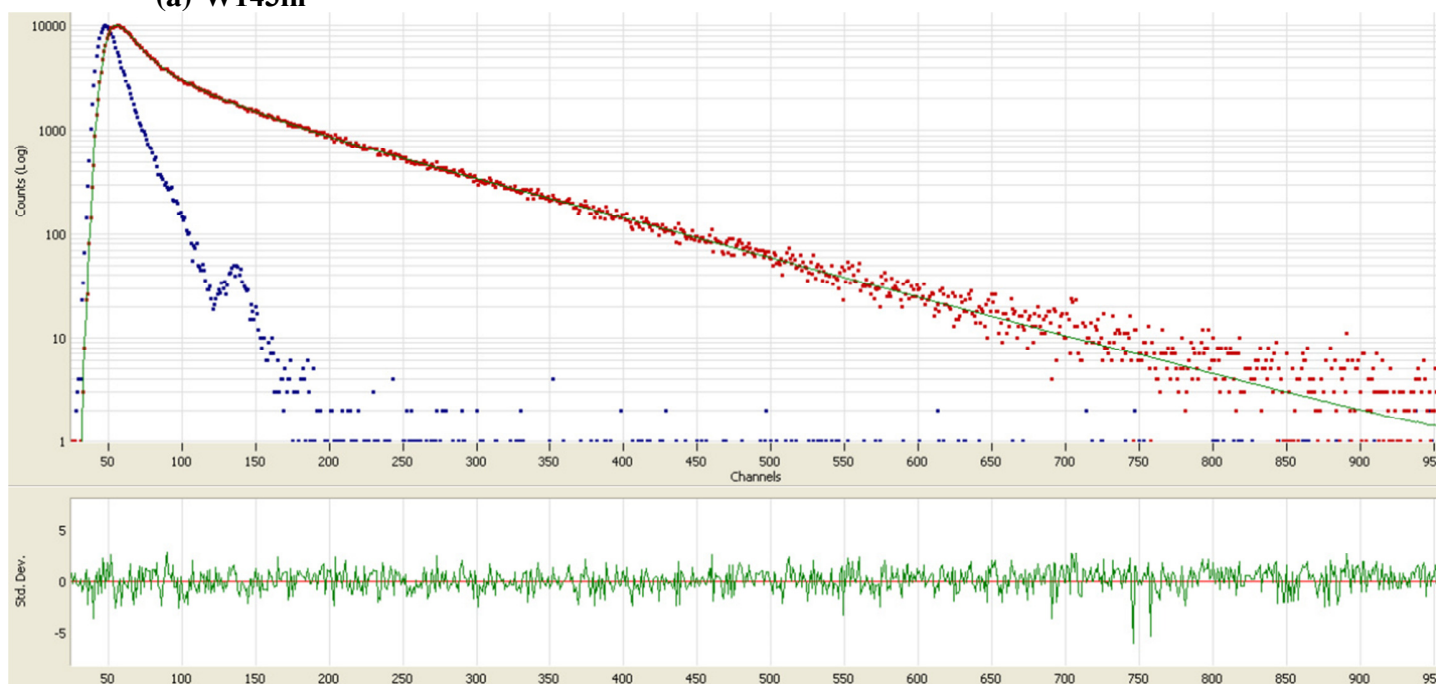
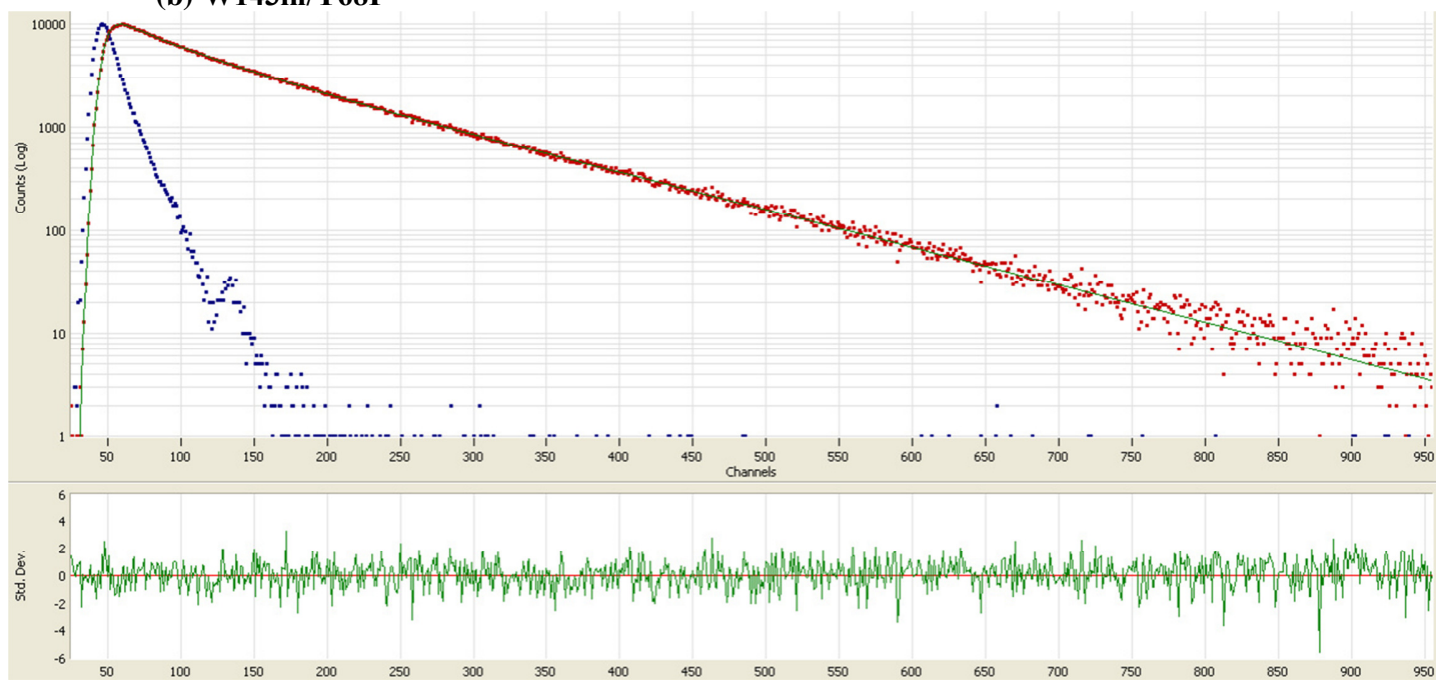


Figure S4. Representative lifetime decays (data in red) with three exponential fit (in green) and residual errors for W143in, W143in/Y68F and W143in/Y68A with AdoMet at 350nm.

(a) W143in



(b) W143in/Y68F



(c) W143in/Y68A

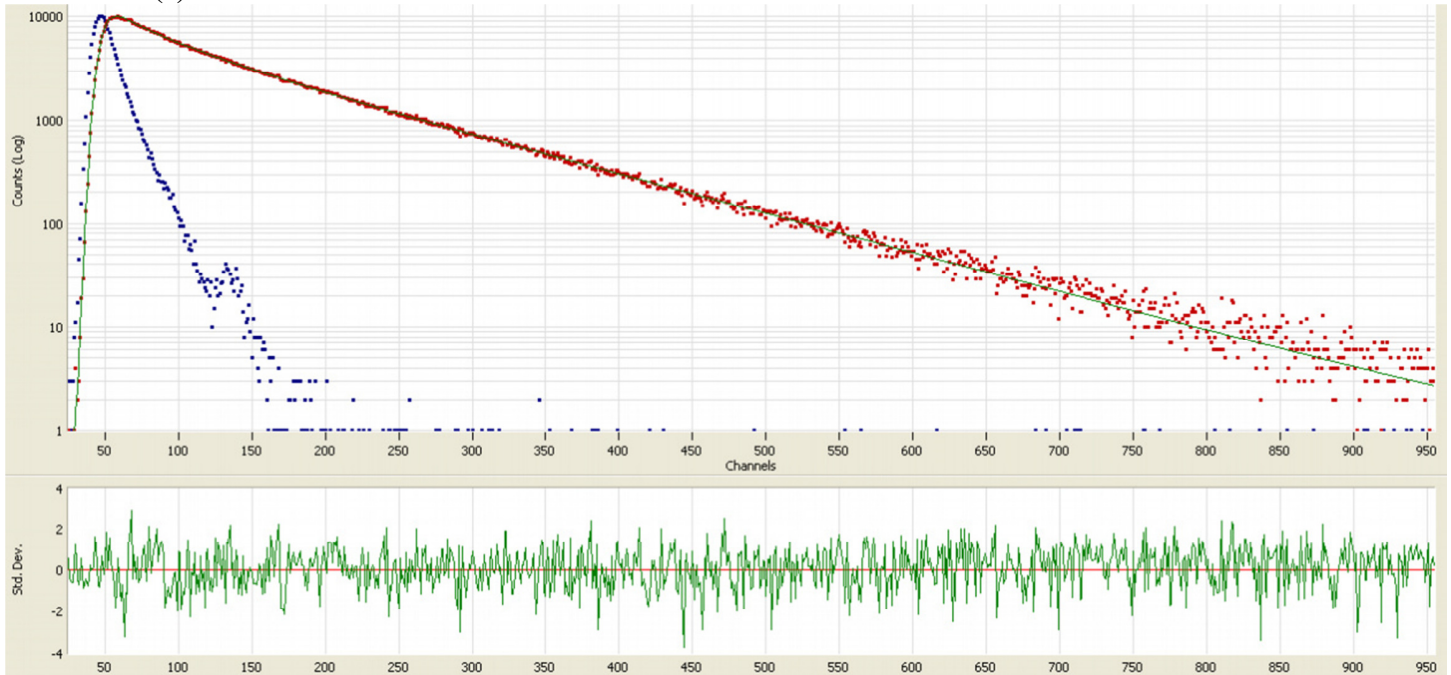


Figure S5. Correlation functions of time-resolved Stokes shift for W143in series with AdoMet: W143in (black), W143in/Y68F (red) and W143in/Y68A (blue).

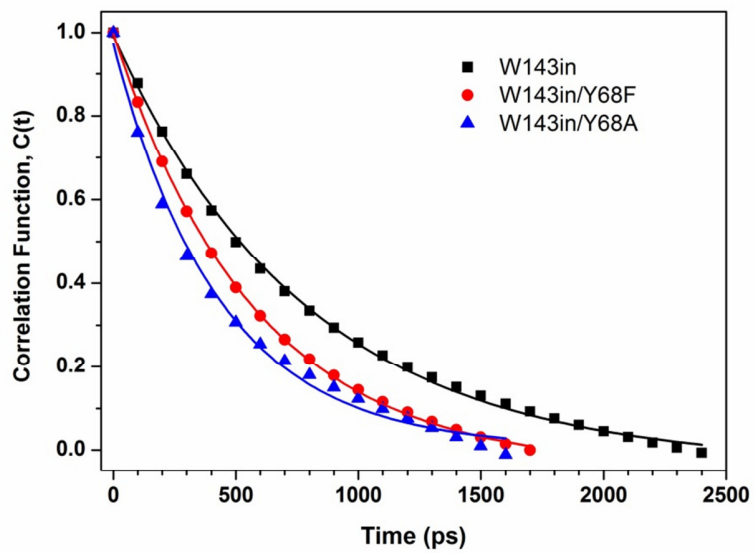


Figure S6. Representative time-resolved emission spectra for the W143in series with AdoMet. Time interval is 100ps with black line as t=0.

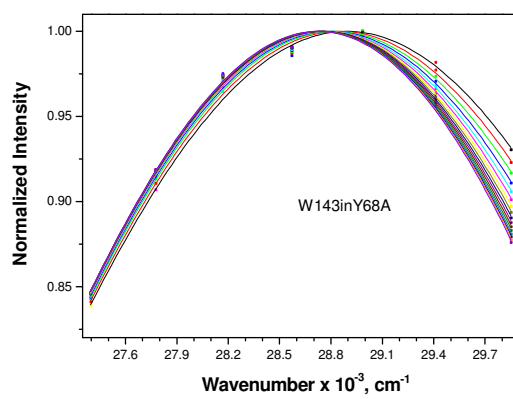
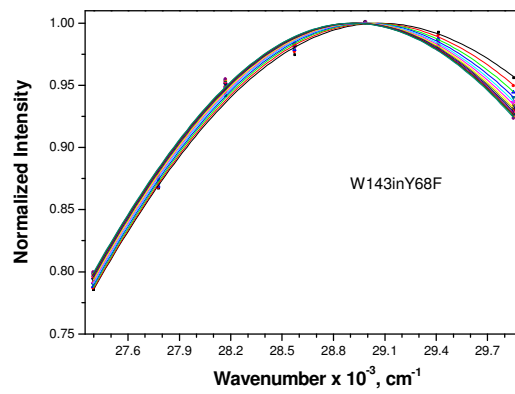
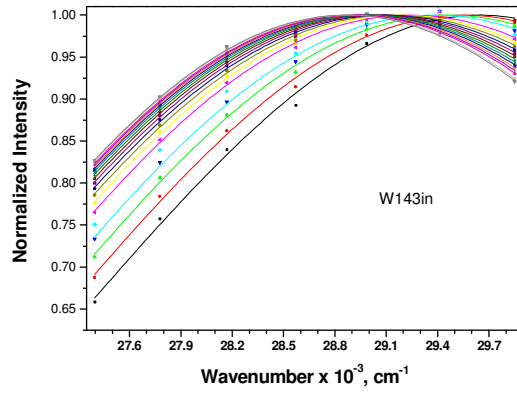
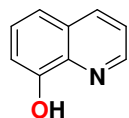
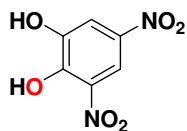


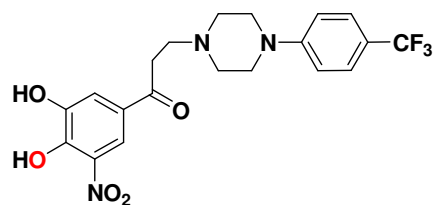
Figure S7. Structure of 8-hydroxyquinoline and inhibitors used in X-ray crystallization in ternary complex studies (**a-e**). Oxygen in red is the atom closer to the carbon of methyl group of AdoMet.



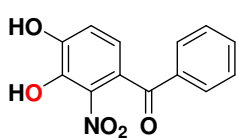
8-hydroxyquinoline



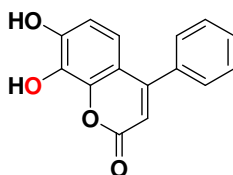
a



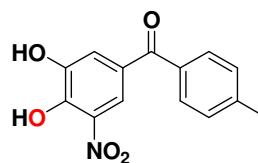
b



c



d



e

Figure S8. pK_a for various catechol and phenol.(21)

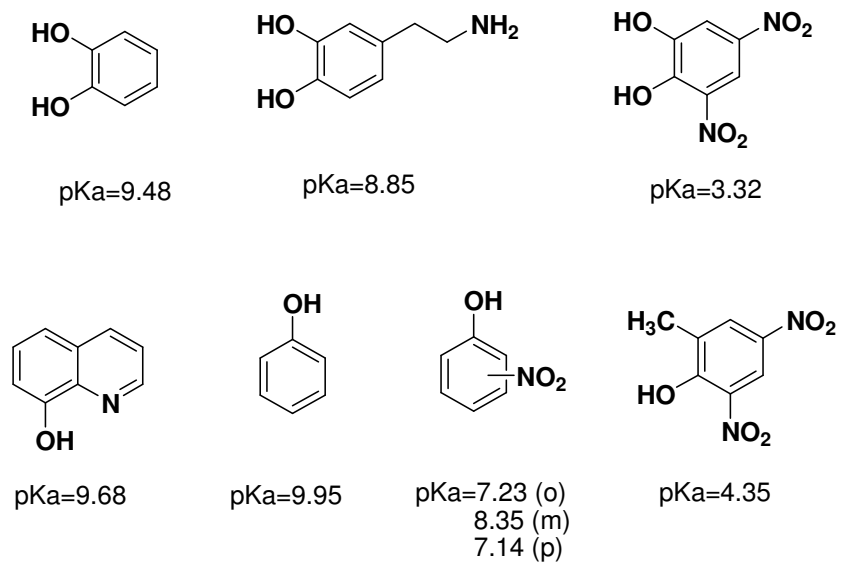


Figure S9. Intramolecular interaction between the AdoMet methyl group to Mg^{2+} (blue dashed lines), and $CH\cdots O$ hydrogen bond (gray dashed lines) in **(a)** binary COMT-AdoMet complex (PDB:2ZTH) and **(b)** in ternary COMT-AdoMet-catechol complex (PDB:3BWM). Distance values (in firebrick) are Angstrom units (underlined).

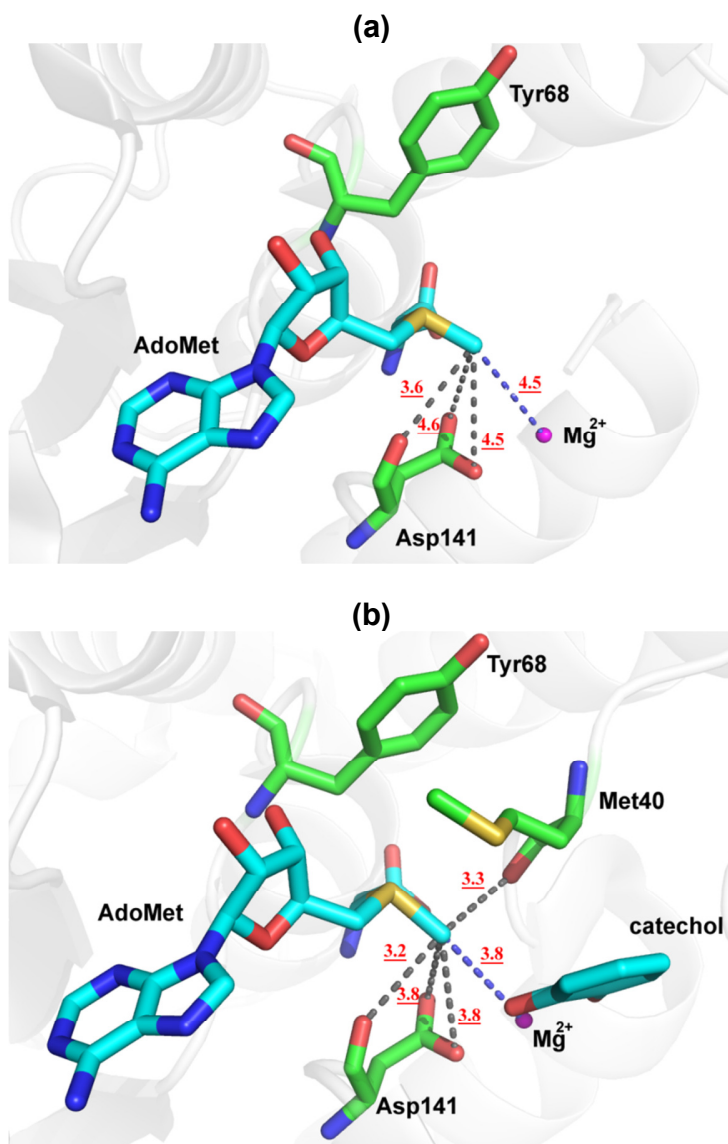


Figure S10. SAM methyl carbon to catecholate O⁻ distance distribution for WT and Y68F and Y68A mutants, derived from MD studies.

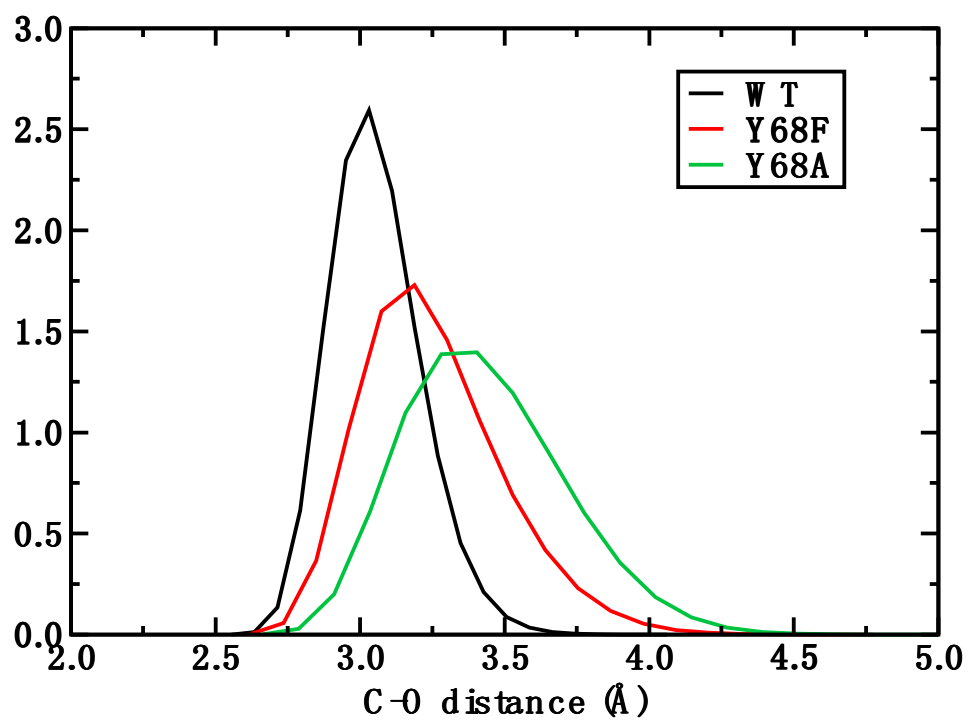
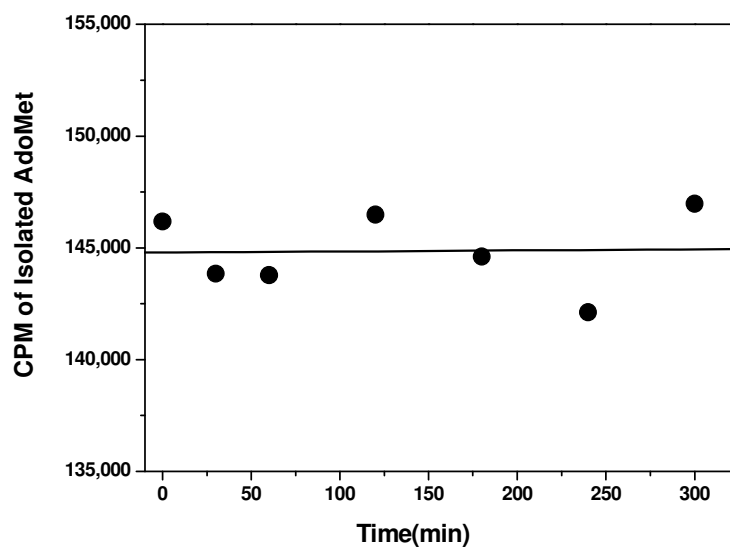


Figure S11. The stability of AdoMet (in the presence of WT COMT) at pH 6.8.



References:

1. Cotton NJH, Stoddard B, & Parson WW (2004) Oxidative inhibition of human soluble catechol-O-methyltransferase. *Journal of Biological Chemistry* 279(22):23710-23718.
2. Rutherford K, Le Trong I, Stenkamp RE, & Parson WW (2008) Crystal Structures of Human 108V and 108M Catechol O-Methyltransferase. *Journal Of Molecular Biology* 380(1):120-130.
3. Dawling S, Roodi N, Mernaugh RL, Wang XH, & Parl FF (2001) Catechol-O-methyltransferase (COMT)-mediated metabolism of catechol estrogens: Comparison of wild-type and variant COMT isoforms. *Cancer Research* 61(18):6716-6722.
4. Zhang J & Klinman JP (2011) Enzymatic Methyl Transfer: Role of an Active Site Residue in Generating Active Site Compaction That Correlates with Catalytic Efficiency. *Journal of the American Chemical Society* 133(43):17134-17137.
5. Zhang J, & Klinman JP (2015) HPLC Separation of the (S,S)- and (R,S)- forms of S-Adenosyl-L-methionine. *Analytical Biochemistry* 476:81-83.
6. Lewis BE & Schramm VL (2003) Binding equilibrium isotope effects for glucose at the catalytic domain of human brain hexokinase. *Journal of the American Chemical Society* 125(16):4785-4798.
7. Murkin AS, *et al.* (2007) Neighboring group participation in the transition state of human purine nucleoside phosphorylase. *Biochemistry* 46(17):5038-5049.
8. Murkin AS, Tyler PC, & Schramm VL (2008) Transition-state interactions revealed in purine nucleoside phosphorylase by binding isotope effects. *Journal of the American Chemical Society* 130(7):2166-2167.
9. Zhang Y & Schramm VL (2011) Ground-State Destabilization in Orotate Phosphoribosyltransferases by Binding Isotope Effects. *Biochemistry* 50(21):4813-4818.
10. Grant KL & Klinman JP (1989) Evidence that both protium and deuterium undergo significant tunneling in the reaction catalyzed by bovine serum amine oxidase. *Biochemistry* 28(16):6597-6605.
11. Hong BY, Maley F, & Kohen A (2007) Role of Y94 in proton and hydride transfers catalyzed by thymidylate synthase. *Biochemistry* 46(49):14188-14197.
12. Bandaria JN, Cheatum CM, & Kohen A (2009) Examination of Enzymatic H-Tunneling through Kinetics and Dynamics. (Translated from English) *Journal of the American Chemical Society* 131(29):10151-10155 (in English).
13. Petrounia IP & Pollack RM (1998) Substituent effects on the binding of phenols to the D38N mutant of 3-oxo-Delta(5)-steroid isomerase. A probe for the nature of hydrogen bonding to the intermediate. *Biochemistry* 37(2):700-705.
14. Meadows CW, Ou R, & Klinman JP (2014) Picosecond-Resolved Fluorescent Probes at Functionally Distinct Tryptophans within a Thermophilic Alcohol Dehydrogenase: Relationship of Temperature-Dependent Changes in Fluorescence to Catalysis. *Journal of Physical Chemistry B* 118(23):6049-6061.
15. Frisch MJ, *et al.* (2009) Gaussian 09 (Gaussian, Inc., Wallingford, CT, USA).
16. Case DA, *et al.* (2012) Amber 12.
17. Petachem. <http://www.petachem.com>.
18. Ditchfield R, Hehre WJ, & Pople JA (1971) Self-Consistent Molecular Orbital Methods. 9. Extended Gaussian-type basis for molecular orbital studies of organic molecules. *Journal of Chemical Physics* 54:724.
19. Kulik HJ, Luehr N, Ufimtsev IS, & Martinez TJ (2012) Ab Initio Quantum Chemistry for Protein Structures. *Journal of Physical Chemistry B* 116(41):12501-12509.
20. Kulik HJ, Zhang J, Klinman JP, & Martínez TJ (2015) How large should the QM region be in QM/MM calculations? The case of catechol O-methyltransferase. arXiv:1505.05730v1 [q-bio.BM]
21. The pKa values are either from Reaxys database (<https://www.reaxys.com/>) or from pKa Data Compiled by R. Williams, (http://research.chem.psu.edu/brpgroup/pKa_compilation.pdf)